Characterization and microhardness of Co–W coatings electrodeposited at different pH using gluconate bath: A comparative study

Parthasarathi Bera[a,*], H. Seenivasan[a], K. S. Rajam[a], C. Shivakumara[b] and Sanjit Kumar Parida[b]

[a]*Surface Engineering Division, CSIR–National Aerospace Laboratories, Bangalore 560017, India*

[b]*Solid State and Structural Chemistry Unit, Indian Institute of Science, Bangalore 560012, India*

Abstract

Electrodeposition of Co–W alloy coatings has been carried out with DC and PC using gluconate bath at different pH. These coatings are characterized for their structure, morphology and chemical composition by XRD, FESEM, DSC and XPS. Alloy coatings plated at pH8 are crystalline, whereas coatings electrodeposited at pH5 are nanocrystalline in nature. XPS studies have demonstrated that as-deposited alloy plated at pH8 with DC contain only Co^{2+} and W^{6+} species, whereas that alloy plated at pH5 has significant amount of Co^{0} and W^{0} along with Co^{2+} and W^{6+} species. Again, Co^{2+} and W^{6+} are main species in all as-deposited PC plated alloys in both pH. Co^{0} concentration increases upon successive sputtering of all alloy coatings. In contrast, mainly W^{6+} species is detected in the following layers of all alloys plated with PC. Alloys plated at pH5 shows higher microhardness compared to their pH8 counterparts.

Keywords: Co–W coating; Gluconate bath; pH variation; XPS

---

*Corresponding author

Tel: +91–80–25086359, Fax: +91–80–25210113, E mail: partho@nal.res.in (P. Bera)

[a]Present address: Department of Chemical Sciences, Indian Institute of Science Education and Research Kolkata, Mohanpur 741252, West Bengal, India

Introduction

Metal alloys have attracted much attention due to their widespread applications in physics, chemistry and engineering for several years. Cobalt and cobalt alloys find their applications in the production of hard materials, magnets, tire adhesives, catalysts, colorants, chemicals, and batteries [1]. Cobalt alloys are unique for their magnetic and mechanical properties, high oxidation stability and wear resistance. The magnetic properties of electrodeposited cobalt alloys are of great interest in electronics applications, especially in the information technology and media industries, where they are used in fabricating permanent data storage devices [2]. Cobalt alloys are also used as anticorrosive protection for aerospace and autobody components production. Among the cobalt alloy materials, Co–W alloys are of great interest due to their exceptional hardness, wear resistance and high corrosion resistance. Moreover, due to high hardness of tungsten alloys, they could successfully substitute hard chromium coatings that are formed in the environmentally hazardous process based on hexavalent chromium [3,4]. The chromates with hexavalent chromium (CrO_3) have been recognized over past 10 years as a highly toxic and carcinogenic chemical [5]. Tungsten metal and its alloys are also used in ultrahigh temperature applications. Again, Co–W is known to have good magnetic property and it has recently been used in integral sensors and inductors.

Electrodeposition is widely recognized as a technologically feasible, economically superior and low temperature technique for fabricating good quality alloys [6–8]. Electrodeposition of tungsten containing alloys is an interesting phenomenon, because it has been observed that tungsten cannot be electrodeposited individually from aqueous electrolyte [9]. However, it could be codeposited from aqueous electrolyte

containing iron group metals (Fe, Co, Ni) and tungstate ion, which is termed as ‘induced codeposition’ [9]. Electrodeposition, surface structure, morphology, composition and properties of Co−W alloys have been studied by several researchers [10–21]. Electrodeposition processes are carried out from baths containing different complexing agents. Citrate electrolyte baths are employed for the electrodeposition of Co–W alloy coatings and it has been observed that composition, structure and properties of these alloy coatings depend on the conditions of electrodeposition [16,17]. Generally, citrate baths are employed in alkaline conditions and formation of surface cracks has been reported in some cases [17,22]. Booze has first introduced the usage of gluconate as a complexing agent in electroless nickel [23]. Since then, gluconate is being used in the area of electro as well as electroless deposition methods. Weston et al. have used gluconate baths to electrodeposite Co–W coatings and extensively investigated different aspects of electrolyte formulations and plating conditions, microstructure, corrosion and wear behaviors [18,19]. However, comprehensive XPS studies on the influence of different electrodeposition parameters such as pH, plating mode, bath composition lack in the literature.

The goal of this present investigation is the deposition of Co–W alloys from gluconate bath with direct current (DC) and pulse current (PC) at pH8 and pH5 and to compare their structure, morphology, composition and microhardness employing X-ray diffraction (XRD), field emission scanning electron microscopy (FESEM), energy dispersive X-ray spectroscopy (EDXS), differential scanning calorimetry (DSC) and X-ray photoelectron spectroscopy (XPS). As the alloy surface composition significantly differs from that of interior layers, surface of these alloys has been sputtered up to few

layers and their compositions as well as elemental oxidation states in each interior layer have been evaluated with XPS.

Materials and methods

Co–W alloy coatings were plated from a bath containing cobalt sulfate heptahydrate (15 g L^{-1}), sodium tungstate dihydrate (16.5 g L^{-1}), boric acid (40 g L^{-1}), sodium gluconate (110 g L^{-1}) and sodium chloride (30 g L^{-1}). The pH of prepared bath was around 5.2 and the pH was adjusted to 8.0 ± 0.05 by the addition of NaOH. Analytical grade chemicals and distilled water were used to prepare the baths. For electrodeposition, approximately 200 mL solution was taken in a 250 mL glass beaker. Temperature of the bath was maintained at 80 °C using a constant temperature water bath. A graphite bar was used as the anode and a brass sheet with 10 cm × 2.5 cm × 0.1 cm dimension was used as the substrate. For XPS and DSC studies plating was done on stainless steel substrates. Substrate was degreased with acetone, rinsed with tap and deionized water, cathodically cleaned with 10 % NaOH solution for 1 min at 15 A dm^{-2}, rinsed with tap and deionized water. Then the substrate was deoxidized with 10 vol.% H_2SO_4 for 30 s (50 vol.% H_2SO_4 for 5 s for stainless steel substrate), rinsed with tap water and deionized water and loaded in the bath for electroplating. Electrodeposition was carried out by DC and PC electrodeposition methods. DC electrodeposition was carried out galvanostatically by using an Aplab 7253 regulated DC power supply. The PC electrodeposition was also carried out galvanostatically using cathodic square wave unipolar double pulse plating rectifier. The DC deposition of Co–W alloy was carried out at an average applied current density of 4.7 A dm^{-2}. The peak current density (i_p) for the pulse deposition was calculated by taking the average current density (i_{av}) as 4.7 A dm^{-2}

and t_{on} as 2 ms and t_{off} as 2, 4 and 8 ms, respectively. Therefore, elecrtodeposition of alloy coatings with pulses of 1:1, 1:2 and 1:4 was carried out at peak current densities of 9.4, 14.1 and 23.5 A dm^{-2}, respectively. The peak current density (i_p) was calculated by using the following equation:

$$i_p = \text{Duty ratio} \times i_{av}, \text{ where Duty ratio} = \frac{t_{on}}{t_{on} + t_{off}}$$

The current efficiency of the deposits has been evaluated by using the following formula

$$\text{Current efficiency} = \frac{Observed\ weight}{Theoretical\ weight} \times 100\ \%$$

The pulse profiles used for different ratios (1:1, 1:2 and 1:4) for electrodeposition is given in Fig. 1. The current efficiencies of the deposits have been evaluated using Faraday's first law of electrolysis with electrochemical equivalence of Co−W as 0.000311 g C^{-1}. The plating was carried out for 1 h and the deposited coating was rinsed with deionized water and dried at room temperature.

The structure of alloy deposits was determined by XRD studies employing a PANalytical X'Pert PRO X-Ray diffractometer operated with CuKα radiation of 1.5418 Å wavelength at 40 kV and 30 mA in the 2θ range 10−80°.

The surface morphology and composition of these alloys were examined by FESEM using a Carl Zeiss Supra 40 V coupled with energy dispersive X-ray spectrometer (EDXS) from Oxford Instruments.

DSC studies for the phase transformation of these Co−W alloys were performed with a Diamond DSC (Perkin Elmer). The sample was taken in the form of a foil and cut into smaller pieces. About 0.5 g sample was put in an aluminium pan and crimped using a cover. Empty aluminium pan with cover crimped was used as a reference. The crimped

specimen and reference samples were placed in a Pt furnace and heated with different heating rates of 10, 20, 30 and 40 °C min^{-1} under continuous purging of the heating chamber with nitrogen flow of 30 mL min^{-1} to avoid sample oxidation. The plot of temperature against heat flow was obtained.

XPS of these Co–W alloy coatings electrodeposited with direct and pulse current were recorded with a Thermo Fisher Scientific Multilab 2000 (England) spectrometer using non-monochromatic AlKα radiation (1486.6 eV) run at 15 kV and 10 mA as X-ray source. The binding energies (E_B) reported here were calculated with reference to C1s peak at 284.5 eV with a precision of ± 0.1 eV. For XPS analysis, thin alloy coatings were mounted on the sample holder after cutting into small pieces and they were kept in the preparation chamber with ultrahigh vacuum (UHV) at 10^{-9} Torr for 5 h in order to desorb any volatile species present on the surface. After 5 h, samples were transferred into the analyzer chamber with UHV at 10^{-9} Torr. All the spectra were obtained with pass energy of 30 eV and step increment of 0.05 eV. Intermittent sputtering was carried out by defocused Ar^+ ion beam using 3 keV EX05 ion gun fitted in the preparation chamber of the spectrometer by applying energy of 3 keV at 2.6 μA beam current over an area of 4 × 4 mm^2 with Ar gas pressure of 5 × 10^{-6} Torr. The experimental data were curve fitted with Gaussian peaks after subtracting a linear background employing PeakFit v4.11 program. For Gaussian peaks, slightly different full width at half maximum (FWHM) was used for different chemical states. The spin-orbit splitting and doublet intensities were fixed as given in the literature [24].

Microhardness measurements of these alloys were carried out on the surface of the deposits using Buehler microhardness tester (Micromet 100) with a Knoop indenter

under a test load of 50 g for 15 s. For microhardness measurements, samples were polished with 0.3 μm Al_2O_3 until mirror finishing was obtained. Average hardness value (HK) was estimated by making 5 indents on each sample.

Results

Current efficiencies, deposition rates and chemical compositions

There are no appreciable changes in the values of current efficiencies and thicknesses of pH8 plated coatings compared to pH5 plated one. Observed values of current efficiencies and coating thickness (deposition rate) are in the range of 62–70% and 36–41 μm h^{-1}, respectively in all the coatings deposited at pH8, whereas these values are 62–66% and 36–30 μm h^{-1} for coatings deposited at pH5.

Compositions of all alloys plated with DC and PC modes at pH8 and pH5 were determined by EDXS studies. There is no significant change in weight as well as atomic percentages of Co and W in DC and PC plated Co–W alloy coatings prepared at pH8. Average weight percentages of Co and W in these alloy deposits are 60 and 40%. On the other hand, Co–W alloys electrodeposited at pH5 contain average Co and W weight percentages of 54 and 46%, respectively.

XRD studies

XRD patterns of as-deposited Co–W alloy coatings prepared at pH8 and pH5 are displayed in Fig. 2. DC and 1:4 PC plated alloy coatings obtained from pH8 show identical XRD patterns, whereas those for 1:1 and 1:2 PC plated coatings are of similar kinds. XRD lines with d values of 2.21, 2.06 (broad), 1.96, 1.85, 1.31 and 1.28 present in

DC and 1:4 PC plated coatings correspond to (200), (002), (201), (102), (103) and (220) planes of Co_3W alloy [25]. Pulse plated 1:1 and 1:2 Co–W films show three main peaks in their XRD patterns. Peaks with d values of 2.21, 1.95 and 1.28 could be attributed to (200), (201) and (220) planes of Co_3W alloy phase. Appearance of Co_3W phase in Co–W coatings electrodeposited at pH8 in this study was observed in the earlier reports on such types of coatings obtained from higher pH [20,26]. The variation of crystallographic orientation and phase component may be due to the different interactions with crystal planes, which induces the different growth mechanism [27]. The formation of amorphous alloy is controlled by the very complicated cathodic process. W cannot be electrochemically deposited on the cathode from the solutions of ions or complex anions. The electrochemical formation of amorphous alloy thin layers is mainly due to a reduction of Co and W on the cathode from highly dispersed combined hydrated Co and W oxides formed in the layer adjacent to the cathode under the influence of hydrogen evolution [28]. The ratio of the hydrated Co and W oxides, in turn, is influenced and determined by the stability of the gluconate complexes in electrolyte. From the XRD patterns of Co–W alloys electrodeposited at pH8 shown in Fig. 2, it is clear that the addition of tungsten to the Co modifies the crystallographic texture. It transforms from the polycrystalline which is regular for pure electrodeposited Co into deformed texture for Co–W alloys. Deformation of the structure causes the slight shifting of the peak position in the XRD patterns. Such shift is characteristic for tungsten alloys [29,30]. A broad peak around 44.5° obtained for all the Co–W alloys electrodeposited at pH5 indicates the amorphous nature of deposits. Similar behavior was observed in Co–W coating electrodepositied with current density of 5 A dm^{-2} at pH6 [18]. Peak intensities in

all samples are more or less same. Grain sizes of these alloy deposits evaluated from Debye-Scherrer method are about 2 nm. Formation of amorphous alloys is the result of deposition of mutually incoherent particles that are too small for crystalline configuration to be formed energetically. In the as-deposited Co–W alloy coatings obtained from electrodeposition with pH5, there is no evidence of the intermetallic compound like Co_3W.

FESEM studies

The surface morphologies of DC plated and PC plated Co–W alloys prepared with electrolyte solution of pH8 and pH5 characterized by FESEM are displayed in Fig. 3. DC and PC electrodeposited Co–W coatings with pH8 contain big spherical nodules on their surfaces. On the other hand, DC and PC deposited Co–W coatings obtained from pH5 consist of spherical and smooth bright nodules over their surfaces. It is clear form the images that the coatings obtained at pH5 are comparatively smoother than the Co–W coatings from pH8. The increase in pH has increased the roughness and also the crystallinity of the coatings. FESEM images seem to support the results obtained from XRD analysis. The roughness of the Co–W coatings at pH8 could also be attributed to the decrease in W content in the deposit. In general, presence of alloying element in a coating decreases the roughness while the amount of alloying element decides the magnitude of roughness. Similar scenario was also observed in Co–W–P deposits obtained from citrate bath [31]. All Co–W alloys are free from microcracks as observed from FESEM images and no deviation from spherical nodular deposits is observed in any of the coatings.

DSC studies

DSC profiles of all Co−W alloy coatings deposited at pH8 are presented in Fig. 4 and no appreciable transitions could be observed in the profiles. This behavior suggests that the alloy coatings are already in crystalline form and further crystallization is not possible in the temperature range used for scanning. This finding agrees well with our XRD results. The thermograms also show that the sample has no retained recovery energy and a reduction in the recrystallisation energy [32]. DSC profiles of Co–W deposits obtained at pH5 with direct and 1:4 pulse current are given for comparison. As seen from the XRD patterns all the coatings electrodeposited with direct and pulse current are amorphous/nanocrystalline which can also be called as a metastable phase. These metastable alloys undergo phase transformation to become completely stable phases. DSC curves of DC and PC electrodeposited Co–W alloy plated at pH5 contain two exothermic peaks at 160 and 322 °C and one endothermic peak at 490 °C. The DSC profiles with higher scanning rates demonstrate that the two exotherms are not major and hence could not be ascribed to the crystallization of any stable phases in the deposits. The presence of these exothermic peaks could be attributed to the internal rearrangement of atoms at these temperatures or structural relaxation such as annihilation of point defects and dislocations within the grains and grain boundary zones. Since the two exothermic peaks present are very shallow and are not very prominent the attention is shifted to the unusual endothermic peak at around 490 °C. The presence of endothermic peak at higher temperature may be due to the partial melting of some of the phases present in Co–W deposit. The endothermic peak observed in the coating might have formed due to increased disorderliness in the coating at this temperature. Increase in disorderliness actually means the increase in entropy of a system. From the definition of

thermodynamics it can be proved that the increase in disorderliness (entropy) of a system is accompanied by heat intake by the system which conforms to the appearance of the endothermic peak.

XPS studies

XPS studies of these alloy coatings could lighten information on the elemental composition and their oxidation states both on the surface and in the bulk up to few layers. Therefore, extensive XPS studies of these alloy coatings have been carried out.

DC electrodeposited Co–W alloy coatings

In Fig. 5, XPS of Co2p core level region in as-deposited DC Co–W alloy coatings prepared at pH8 and the same sample after 10, 20 and 30 min sputtering are shown. In the same figure, XPS of Co2p of as-deposited DC Co–W alloy plated at pH5 is also shown for comparison. Accordingly, in the as-deposited sample, $Co2p_{3/2,1/2}$ peaks at 781.8 and 797.3 eV having spin-orbit separation [ΔE_B ($2p_{3/2}$–$2p_{1/2}$)] of 15.5 eV along with strong satellite peaks at 4.2 and 6.3 eV higher energy in relation to main peaks could be attributed to Co^{2+} from highly ionic Co^{2+} type of species present in this kind of alloy coatings [33–35]. Envelop of $Co2p_{3/2,1/2}$ after successive sputtering is broader compared to as-deposited sample indicating that Co is present in several oxidation states. Spectra could be deconvoluted into sets of spin-orbit doublets along with associated satellite (S) peaks. A typical deconvoluted spectrum of Co2p in the sample after 30 min sputtering is shown in Fig. 6. In contrast, both Co metal and Co^{2+} species could be observed in as-deposited Co–W alloy electrodeposited with direct current in the electrolyte solution of pH5. In this alloy coating, $Co2p_{3/2,1/2}$ peaks at 778.3 and 793.1 eV with spin-orbit separation of 14.8 eV correspond to Co metal, whereas peaks at 781.7 and 797.6 eV with

15.9 eV spin-orbit separation could be attributed to Co^{2+}. It has been observed that oxidized Co species is seen to be the predominated species along with little amount of Co metal in the subsequent layers even after 30 min sputtering of all type of samples except DC plated alloy electrodeposited at pH5 where Co metal starts to become the main species after 10 min sputtering. The binding energies, relative intensities and FWHMs of different Co species as observed from Co2p spectra of Co–W alloys prepared with DC at pH8 and pH5 at different stages of sputtering are summarized in Tables 1 and 2, respectively.

X-ray excited Auger electron spectroscopy (XAES) of CoL_3VV was also carried out to get insight into nature of Co species during several stages of sputtering of DC alloy electodeposited at pH8 and it is shown in Fig. 7. As-deposited coating shows a peak at 770.0 eV that corresponds to Co^{2+} species only [36,37]. Upon sputtering higher kinetic energy peak at 771.5 eV gets slowly developed that could be related to metallic Co species indicating the formation of metallic component in the successive layers. Shift of oxidized peak to lower binding energy at 767.8 eV is also observed during sputtering. Hence, XAES results obtained in the present alloy coating agree well with XPS findings. CoL_3VV of as-deposited coating consists of peaks at 773.0 and 765.0 eV corresponding to Co metal, CoO species respectively [36,37]. Upon sputtering a sharp peak at 773.0 eV is observed indicating the existence of more amount of Co metal in the successive layers.

XPS of W4f core level region in different sputtering conditions in DC plated Co–W alloy coatings prepared at pH8 are displayed in Fig. 8. XPS of W4f of as-deposited DC plated Co–W alloy coating prepared at pH5 is also shown in the same figure for comparison. There could be several W components in as-deposited Co–W

alloys as seen from the features of W4f envelop. Fig. 9 shows deconvoluted W4f spectrum of as-deposited DC alloy plated at pH8. Deconvoluted spectrum shows intense $W4f_{7/2,5/2}$ peaks at 36.2 and 38.3 eV corresponding to W^{6+} state [13,34], whereas there is a signature of very weak broad hump in 29–34 eV binding energy region that comprises the components of metallic W as well as Na2p. Accordingly, $W4f_{7/2,5/2}$ peaks at 31.0 and 33.0 eV could be assigned to metallic W species only [13,34]. Peak around 31.7 eV could be ascribed to Na2p that comes from the bath as it contains Na salt [38,39]. Decrease in the intensity of this broad peak region could be seen upon successive sputtering. On the other hand, $W4f_{7/2,5/2}$ peaks are observed at 31.4, 33.6 and 36.1 and 38.2 eV in case of the as-deposited DC Co–W sample prepared at pH5 that correspond to W^0 and W^{6+} species, respectively. It important to mention that the intensities of 29–34 eV binding energy region peaks are much more in the alloy plated at pH5 compared to alloy plated at pH8. Peak related to Na2p could not be observed in alloy plated at pH5 as intensity ratio of $W4f_{7/2}$ to $W4f_{5/2}$ obtained from the experiment agrees well with theoretical value. Metallic W concentration increases slowly upon sputtering of the alloy electrodeposited at pH5. The binding energies, relative intensities and FWHMs of different W species as observed from W4f spectra of Co–W alloys prepared at pH8 and pH5 subjected to intermittent sputtering are summarized in Tables 3 and 4, respectively.

PC electrodeposited Co–W alloy coatings

XPS of Co–W alloys electrodeposited with different pulse current of 1:1, 1:2 and 1:4 at pH8 are also carried in our present study and in Fig. 10, XPS of Co2p core level of as-deposited Co–W alloy under 1:4 pulse current including the same after 10, 20 and 30 min sputtering is displayed. In the same figure, XPS of Co2p of as-deposited 1:4 PC

Co–W alloy plated at pH5 is also shown for comparison. In all cases, spectra could be deconvoluted into sets of spin-orbit doublets along with their respective satellite peaks. Accordingly, XPS of as-deposited Co–W alloy plated with 1:1 pulse current at pH8 contains $Co2p_{3/2,1/2}$ peaks at 781.7 and 797.5 eV, whereas two sets of $Co2p_{3/2,1/2}$ spin-orbit doublet peaks at 778.3, 793.4 and 781.5, 797.1 eV could be observed in 1:2 PC plated film. Again, $Co2p_{3/2,1/2}$ peaks at 781.6 and 797.3 eV are observed in the as-deposited alloy plated with 1:4 PC at pH8. Lower binding energy doublet peaks with very low concentration present in 1:2 PC plated alloy are related to Co metal. On the other hand, higher binding energy sets observed in all alloys could only be attributed to metallic Co^{2+} species. Slow increase in the concentration of Co metal with sputtering is observed for the above samples. XPS studies Co–W alloys electrodeposited with different pulse current of 1:1, 1:2 and 1:4 at pH5 show similar kind of results. Mainly Co^{2+} species is observed to be seen in all alloys, 1:2 and 1:4 PC plated alloys show little amount of Co metal species. In 1:4 PC plated alloy electrodeposited at pH5, $Co2p_{3/2,1/2}$ peaks at 778.1 and 793.2 eV could be assigned to metallic Co species, whereas peaks at 781.5 and 797.0 could be ascribed to Co^{2+}, but concentration of Co^{2+} species is much more in comparison with Co metal. Significant amount of Co metal is seen with sputtering of the subsequent layers in the above samples. Thus, there are differences in concentration of various Co species prepared at pH8 and pH5. The binding energies, relative intensities and FWHMs of different Co species as observed from Co2p spectra of Co–W alloys prepared with DC and 1:4 PC at pH8 and pH5 at different stages of sputtering are summarized in Table 5 and 6, respectively.

In XAES of CoL_3VV of all alloys plated at pH8 with pulse current, broad features between 760 and 780 eV could be observed. As-deposited alloy shows a hump around 767.5 eV indicating the presence of Co^{2+} species. There is also a clear indication of the presence of higher kinetic energy peak around 772.7 eV upon sputtering indicating presence of Co metal in the interior layers.

XPS of W4f core level regions in 1:1, 1:2 and 1:4 PC plated alloys electrodeposited at pH8 demonstrate the presence of mainly W^{6+} species. A small very less intense broad peak in 29–34 eV binding energy region could also be observed in all alloys that contains components of W^0 and Na2p. Na2p peak is related to Na salt taken for the preparation. This lower binding peak intensity decreases upon sputtering in all alloys except 1:2 PC plated alloy. In contrast, PC plated alloys prepared at pH5 contain W^{6+} species only that does not change during sputtering. Details of the binding energies, relative intensities and FWHMs of different W species as observed from W4f spectra of 1:4 PC plated Co–W alloys prepared at pH8 and pH5 subjected to intermittent sputtering are summarized in Tables 7 and 8, respectively.

Relative surface concentration

Relative surface concentrations (at.%) of Co and W of as-deposited and sputtered alloys electrodeposited at pH8 and pH5 have been estimated by the relation [40]:

$$\frac{C_{Co}}{C_W} = \frac{I_{Co}\,\sigma_W\,\lambda_W\,D_W}{I_W\,\sigma_{Co}\,\lambda_{Co}\,D_{Co}}$$

where C, I, σ, λ and D are the surface concentration, intensity, photoionization cross-section, mean escape depth and analyzer detection efficiency, respectively. Integrated intensities of Co2p and W4f peaks have been taken into account to estimate the concentration, whereas photoionization cross-sections and mean escape depths have been

obtained from the literature [41,42]. The geometric factor was taken as 1, because the maximum intensity in this spectrometer is obtained at 90^{o}. Accordingly, Relative surface concentrations (at.%) of Co and W in direct current and pulse current plated Co−W alloys prepared at pH8 and pH5 are shown in Table 9.

Microhardness studies

Microhardness measurements of all Co–W alloy deposits plated at pH8 and pH5 were carried out on the surface of as-deposited alloys and the values are given in Table 10. As-deposited Co–W alloys plated at pH8 exhibit average hardness value of 370 HK, whereas coatings electrodeposited with pH5 have average hardness value of 500 HK. The hardness obtained is higher than electrodeposited Co (~300 HK) and the values are higher than the values obtained by Eskin and coworkers [3]. On the other hand, hardness values in the present study are less compared to the values reported by Weston et al. [18] and Su et al. [43]. They got a hardness value of about 1000 kgf mm^{-2} for Co–W coating obtained from citrate bath using reverse pulse plating technique and this was attributed to smaller grain size, higher tungsten content and strong hcp (100) orientation of the Co–W coating. The report by Weston et al. pointed out that the major contribution to the hardness (550 kgf mm^{-2}) of the 20–25 at.% W alloys came from the metastable amorphous phase in which the tungsten atoms were distributed randomly [18]. However, in this study, we find that at pH5, the Co–W coatings are amorphous and exhibit almost similar hardness. Larger grain size in pH8 plated coatings might be the reason for lower hardness. The increase in hardness in alloy deposit in comparison with Co electrodeposit is due to the incorporation of hard material such as tungsten into Co. Differences in microhardness in the alloy coatings electrodeposited with different pH could be due the

presence of different amount of alloyed species in the coatings as well as microstructure of the coatings. In this sense, it could be generalized that the microstructure has a larger impact in determining the property of a coating.

Discussion

In the present study, we have investigated surface structure, morphology and composition of Co−W alloys electrodeposited with direct and pulse current at pH8 using gluconate bath. We have also studied effect of different pH on their surface structure, morphology and composition. Co−W alloys electrodeposited at pH8 are crystallized mainly in Co_3W phase, whereas pH5 plated alloys are amorphous with hcp phase of Co having grain sizes in the range of 2 nm. Surface morphology studies show that alloys are free from microcracks and they are smooth at pH5 and relatively very rough at pH8. Microhardness increases in these alloy deposits compared to Co metal and varies with respect to amount and chemical states of W. The formation of Co–W alloys and amount of codeposited W with Co during electrochemical process depends on electrolyte pH. From EDXS studies, the weight percentage of cobalt and tungsten in the deposit obtained at pH8 is 60 and 40 wt.% while it is 54 and 46 wt.% in the case of the deposits from pH5. The content of W in the electrodeposited Co–W alloy deposits is 46–40 wt.% when pH5 is varied from 5 to 8. The decrease of the electrolyte pH to 5 causes the increase of W content in the alloy to 46 wt.%. A decrease in tungsten content with decrease in pH in the citrate containing baths is reported earlier [44]. In our study, elevation of electrolyte pH to 8 causes the decrease of W content to 40 wt.%. Such changes in tungsten content in the alloy are due to the different stability of Co and W borogluconate complexes. Moreover,

during the electrodeposition of W alloys, the electroreduction of WO_4^{2-} to W is associated with an increase of the pH in the double layer which is as follows:

$$WO_4^{2-} + 4H_2O + 6e \rightarrow W + 8OH^-$$

In addition, the electrodeposition of W alloys is accompanied by H_2 evolution that is given below:

$$2H_2O + 2e \rightarrow H_2 + 2OH^-$$

That yields an alkalization of the electrochemical double layer, what in general decreases the W content in the electrodeposited alloys [30,34,45].

Microstructural studies by XRD shows that Co_3W phase has been formed in the coatings electrodeposited at pH8. On the other hand, coatings obtained with pH5 shows hexagonal Co phase which is the major component of Co–W alloy. From extensive XPS studies of Co2p and W4f core levels in all alloy coatings clearly demonstrate that nature of surface species and their compositions in Co–W alloy deposits vary with current modes as well as pH of bath during electrodeposition. As-deposited DC plated alloy deposit prepared at pH8 contains Co^{2+} species only, whereas Co–W alloy eletrodeposited at pH5 with direct current shows the presence of significant amount of Co metal along with Co^{2+} species. On the other hand, alloy deposits prepared with different pulse current and different pH contain mostly Co^{2+} species with very little amount of Co metal. Co^{2+} species in all alloys could be due to CoO or $Co(OH)_2$. $Co(OH)_2$ might be present on the surface of the alloys as alkalization of the electrolyte occurs at the cathode layer due to hydrogen evolution during electrodeposition [30,34,45]. This could be substantiated from the core level O1s spectra. XPS of O1s core level region of both as-deposited coatings

reveal that spectra could be deconvoluted into several peaks as spectral envelop are broad in nature. Deconvoluted O1s spectrum of as-prepared coating obtained from pH8 is shown in Fig. 11. The as-deposited sample shows main peak at 532.2 eV that corresponds to oxygen associated with OH, whereas small peaks at 530.8 and 533.7 eV could represent oxygen corresponding to CoO and H_2O species associated with the sample respectively [46]. The peak at 535.9 eV that could correspond to NaKLL peak deposited on the surface from the solution [39]. Intensity of lower binding energy peak associated with CoO increases with sputtering and it becomes the main species. However, W^{6+} species could be assigned for WO_3 in all deposits. There could be possibility of the formation of mixed $CoWO_4$ in the alloy deposits. It is important to note that Co^{2+} and W^{6+} are the main species in alloy coating electrodeposited with direct current at pH8 in different stages of sputtering, whereas pH5 plated alloy electrodeposited with direct current contains comparatively much more Co and W metallic species along with their oxides during sputtering. However, Co^{2+} is the predominant species in pulse current plated films at pH8 and pH5 in all stages of sputtering. Again, oxide of tungsten is the only tungsten species even after 30 min sputtering of these alloys in case of pH5 plated alloys prepared with pulse current in contrast to pH8 plated alloys where some amount of metallic W is present. Relative surface concentration evaluated from XPS demonstrates that Co is segregated on the surface of all alloys electrodeposited at pH8 and pH5 and it is observed that 1:2 PC plated alloys in both pH has lowest amount of W. There might also be formation of intermetallic phases on the surface or subsurface regions according to the Co and W concentrations. However, there is no significant change of Co and W

concentrations in all alloy deposits upon successive sputtering (Table 9) indicating that alloy coatings have uniform composition up to certain layers.

It has been observed that microhardness is more in case of pH5 plated alloys in comparison with pH8 plated alloys. Alloys electrodeposited at pH8 show average microhardness of 370 HK, whereas that of pH5 plated alloys is 500 HK. This difference is mainly attributed to the nanocrystalline or amorphous nature of alloys exhibited by alloy coatings electrodeposited at pH5. Usually nanocrystalline deposits exhibit higher microhardness compared to their crystalline counterparts. Relative surface concentrations evaluated from XPS demonstrate that pH8 plated coatings have average lower amount of W compared to its pH5 counterparts. Therefore, higher microhardness observed in coatings electrodeposited with pH5 could also be due to presence of more amount of W in relation to pH8 plated coatings. Again, alloy coating plated with DC contains highest W concentration among DC and PC plated coatings obtained with pH5 according to XPS studies, but 36% of its W is in metallic form (see Table 4). Therefore, relatively lower microhardness observed in coating electrodeposited with DC at pH5 could be due to the presence of less amount of alloyed W.

Conclusions

Co–W alloys were deposited with DC and PC modes at pH8 and pH5 using gluconate bath. XRD patterns indicate that alloys electrodeposited at pH8 are crystalline in nature, whereas alloys plated with pH5 are nanocrystalline with 2 nm grain size. There is no significant transition in DSC profiles of alloys plated at pH8, but exothermic and endothermic peaks could be observed in alloys plated at pH5. XPS studies have confirmed the presence of only Co^{2+} and W^{6+} species in as-deposited alloy plated at pH8

with DC, whereas in the alloy plated at pH5 contains appreciable amount of Co^0 and W^0 along with Co^{2+} and W^{6+} species. But, in all as-deposited PC plated alloys prepared at both pH, Co^{2+} and W^{6+} are seen to be the main species. Co^{2+} species in all alloys could be due to the presence of CoO or $Co(OH)_2$ and W^{6+} species could be related to WO_3. Relative surface concentration evaluated from XPS shows that Co is segregated over the surface in all alloys prepared at pH8 and pH5. Upon successive sputtering of all films Co metal concentration increases. On the other hand, mainly W^{6+} species is present in the interior layers of all alloys plated with PC. Alloys electrodeposited at pH5 shows higher microhardness compared to alloys plated at pH8. This could be due to observed nanocrystallinity and incorporation of more amount of hard W material in alloys plated at pH5 compared with alloys electrodeposited at pH8.

Acknowledgements

Authors would like to thank the Director, CSIR–National Aerospace Laboratories for giving permission to publish this work. Authors wish to acknowledge the help rendered by Mr. Siju, Mr. Manikandanath and Mr. Praveen for carrying out FESEM, DSC and microhardness measurements, respectively. Authors are thankful to Prof. M.S. Hegde, Indian Institute of Science, Bangalore for providing XPS facility.

References

[1] Y. Sverdlov, V. Bogush, H. Einati, Y. Shacham-Diamand, *J. Electrochem. Soc.* **2005**, *152*, C631.

[2] K. M. Ismail, W. A. Badawy, *J. Appl. Electrochem.* **2000**, *30*, 1303.

[3] S. Eskin, O. Berkh, G. Rogalsky, J. Zahavi, *Plat. Surf. Finish.* **1998**, *85(4)*, 79.

[4] D. P. Weston, P. H. Shipway, S. J. Harris, M. K. Cheng, *Wear* **2009**, 267, 934.

[5] J. H. Lindsay, *Plat. Surf. Finish.* **1995**, *82(2)*, 19.

[6] J. -X. Kang, W. -Z. Zhao, G. -F. Zhang, *Surf. Coat. Technol.* **2009**, *203*, 1815.

[7] M. Srivastava, V. K. W. Grips, K. S. Rajam, *Appl. Surf. Sci.* **2007**, *253*, 3814.

[8] A. A. Aal, S. M. El-Sheikh, Y. M. Z. Ahmed, *Mater. Res. Bull.* **2009**, *44*, 151.

[9] A. Brenner, Electrodeposition of Alloys: Principles and Practices, Academic Press, New York, 1963.

[10] U. Admon, M. P. Dariel, E. Grünbaum, *J. Appl. Phys.* **1986**, *59*, 2002.

[11] V. G. Shadrow, A. V. Boltushkin, T. A. Tochitskii, L. B. Sosnovskaja, *Thin Solid Films* **1991**, *202*, 61.

[12] M. Donten, Z. Stojek, *J. Appl. Electrochem.* **1996**, *26*, 665.

[13] M. Donten, *J. Solid State Electrochem.* **1999**, *3*, 87.

[14] M. A. M. Ibrahim, S. S. A. El Rehim, S. O. Moussa, *J. Appl. Electrochem.* **2003**, *33*, 627.

[15] Z. A. Hamid, *Mater. Lett.* **2003**, *57*, 2558.

[16] N. I. Tsyntsaru, S. S. Belevskii, G. F. Volodina, O. L. Bersirova, Yu. S. Yapontseva, V. S. Kublanovskii, A. I. Dikusar, *Surf. Eng. Appl. Electrochem.* **2007**, *43*, 312.

[17] S. S. Belevskii, N. I. Tsyntsaru, A. I. Dikusar, *Surf. Eng. Appl. Electrochem.* **2010**, *46*, 91.

[18] D. P. Weston, S. J. Harris, P. H. Shipway, N. J. Weston, G. N. Yap, *Electrochim. Acta* **2010**, *55*, 5695.

[19] D. P. Weston, S. J. Harris, H. Capel, N. Ahmed, P. H. Shipway, J. M. Yellup, *Trans. Inst. Met. Finish.* **2010**, *88*, 47.

[20] M. Mulukutla, V. K. Kommineni, S. P. Harimkar, *Appl. Surf. Sci.* **2012**, *258*, 2886.

[21] F. -H. Su, C. -S. Liu, P. Huang, *Appl. Surf. Sci.* **2012**, *258*, 6550.

[22] H. Cesiulis, X. Xie, E. Podlaha-Murphy, *Mater. Sci. (Medžiagotyra)* **2009**, *15*, 115.

[23] C. A. Booze, *Trans. Inst. Met. Finish.* **1975**, *53*, 49.

[24] D. Briggs, M.P. Seah, Practical Surface Analysis by Auger and X-ray Photoelectron Spectroscopy, Wiley, New York, 1984.

[25] A. Magnéli, A. Westgren, *Z. Anorg. Allg. Chem.* **1938**, *238*, 268.

[26] G. Wei, H. Ge, X. Zhu, Q. Wu, J. Yu, B. Wang, *Appl. Surf. Sci.* **2007**, *253*, 7461.

[27] E. Budevski, G. Staikov, W.J. Lorenz, Electrochemical Phase Formation and Growth, VCH, Weinheim, 1996.

[28] Y. Iyoko, S. Haruyama, *J. Jpn. Inst. Met.* **1989**, *53*, 100.

[29] M. Donten, Z. Stojek, J. G. Osteryoung, *J. Electrochem. Soc.* **1993**, *140*, 3417.

[30] M. Donten, H. Cesiulis, Z. Stojek, *Electrochim. Acta* **2000**, *45*, 3389.

[31] S. M. S. I. Dulal, C. B. Shin, J. Y. Sung, C. -K. Kim, *J. Appl. Electrochem.* **2008**, *38*, 83.

[32] B. M. Hogan, Proc. SUR/FIN 84, American Electroplaters and Surface Finishers Soc., Orlando, Florida, 1984.

[33] N. S. Mclntyre, M. G. Cook, *Anal. Chem.* **1975**, *47*, 2208.

[34] L. Orlovskaja, E. Matulionis, A. Timinskas, V. Šukienė, *Surf. Coat. Technol.* **2000**, *135*, 34.

[35] C. N. R. Rao, D. D. Sarma, S. Vasudevan, M. S. Hegde, *Proc. R. Soc. Lond. A* **1979**, *367*, 239.

[36] J. Haber, L. Ungier, *J. Electron Spectrosc. Relat. Phenom.* **1977**, *12*, 305.

[37] T. Mathew, S. Shylesh, B. M. Devassy, M. Vijayaraj, C. V. V. Satyanarayana, B. S. Rao, C. S. Gopinath, *Appl. Catal. A* **2004**, *273*, 35.

[38] I. C. Lekshmi, A. Gayen, V. Prasad, S. V. Subramanyam, M. S. Hegde, *Mater. Res. Bull.* **2002**, *37*, 1815.

[39] C. D. Wagner, W. M. Riggs, L. E. Davis, J. F. Moulder, in Handbook of X-ray Photoelectron Spectroscopy, (Ed. G.E. Mullenberg), Perkin-Elmer Corporation, Eden Prairie, Minnesota, 1979, p. 184.

[40] C. J. Powell, P. E. Larson, *Appl. Surf. Sci.* **1978**, *1*, 186.

[41] J. H. Scofield, *J. Electron Spectrosc. Relat. Phenom.* **1976**, *8*, 129.

[42] D. R. Penn, *J. Electron Spectrosc. Relat. Phenom.* **1976**, *9*, 29.

[43] F. Su, P. Huang, *Mater. Chem. Phys.* **2012**, *134*, 350.

[44] I. Vītiņa, V. Belmane, A. Krūmiņa, M. Lubāne, *Open Surf. Sci. J.* **2010**, *2*, 1.

[45] H. Cesiulis, A. Baltutiene, M. Donten, M. L. Donten, Z. Stojek, *J. Solid State Electrochem.* 2002, 6, 237.

[46] C. R. Brundle, T. J. Chuang, D. W. Rice, *Surf. Sci.* **1976**, *60*, 286.

Table 1. Binding energies, relative intensities and FWHMs of different Co species as observed from Co2p of as-deposited and sputtered DC Co–W coating prepared at pH8

Duration of sputtering (min)	Co species	E_B of $Co2p_{3/2}$ (eV)	Relative intensity (%)	FWHM of $Co2p_{3/2}$ (eV)	ΔE_B ($2p_{3/2}$–$2p_{1/2}$) (eV)	ΔE_B ($2p_{3/2}$–S) (eV)
As-deposited	Co^0	–	–	–	–	–
	Co^{2+}	781.8	100	2.59	15.5	4.2
10	Co^0	778.3	6	2.65	15.0	–
	Co^{2+}	781.8	94	3.29	15.8	4.7
20	Co^0	778.4	9	2.21	15.3	–
	Co^{2+}	781.6	91	3.66	15.9	4.8
30	Co^0	778.4	18	2.26	15.1	–
	Co^{2+}	781.4	82	3.54	15.7	4.6

Table 2. Binding energies, relative intensities and FWHMs of different Co species as observed from Co2p of as-deposited and sputtered DC Co–W coating prepared at pH5

Duration of sputtering (min)	Co species	E_B of $Co2p_{3/2}$ (eV)	Relative intensity (%)	FWHM of $Co2p_{3/2}$ (eV)	ΔE_B ($2p_{3/2}$–$2p_{1/2}$) (eV)	ΔE_B ($2p_{3/2}$–S) (eV)
As-deposited	Co^0	778.3	26	1.89	14.8	–
	Co^{2+}	781.7	74	3.04	15.9	4.3
10	Co^0	778.4	52	1.85	15.0	–
	Co^{2+}	781.3	48	3.82	15.7	4.7
20	Co^0	778.4	61	1.95	15.0	–
	Co^{2+}	781.4	39	3.88	15.6	4.9
30	Co^0	778.4	67	1.82	15.0	–
	Co^{2+}	781.1	33	4.58	16.0	5.0

Table 3. Binding energies, relative intensities and FWHMs of different W species as observed from W4f of as-deposited and sputtered DC Co–W coating prepared at pH8

Duration of sputtering (min)	W species	E_B of $W4f_{7/2}$ (eV)	Relative intensity (%)	FWHM of $W4f_{7/2}$ (eV)
As-deposited	W^0	31.0	6	1.35
	W^{6+}	36.2	94	1.63
10	W^0	31.1	6	1.40
	W^{6+}	36.3	94	1.55
20	W^0	31.0	4	1.34
	W^{6+}	36.3	96	1.59
30	W^0	31.1	4	1.41
	W^{6+}	36.2	96	1.68

Table 4. Binding energies, relative intensities and FWHMs of different W species as observed from W4f of as-deposited and sputtered DC Co–W coating prepared at pH5

Duration of sputtering (min)	W species	E_B of $W4f_{7/2}$ (eV)	Relative intensity (%)	FWHM of $W4f_{7/2}$ (eV)
As-deposited	W^0	31.4	36	1.36
	W^{6+}	36.1	64	1.83
10	W^0	31.4	37	1.49
	W^{6+}	36.0	63	1.96
20	W^0	31.5	41	1.49
	W^{6+}	36.0	59	1.89
30	W^0	31.6	47	1.49
	W^{6+}	36.0	53	2.03

Table 5. Binding energies, relative intensities and FWHMs of different Co species as observed from Co2p of as-deposited and sputtered 1:4 PC Co–W coating prepared at pH8

Duration of sputtering (min)	Co species	E_B of $Co2p_{3/2}$ (eV)	Relative intensity (%)	FWHM of $Co2p_{3/2}$ (eV)	ΔE_B ($2p_{3/2}$–$2p_{1/2}$) (eV)	ΔE_B ($2p_{3/2}$–S) (eV)
As-deposited	Co^0	–	–	–	–	–
	Co^{2+}	781.6	100	2.91	15.7	4.2
10	Co^0	778.3	5	2.25	14.9	–
	Co^{2+}	781.9	95	3.21	15.8	4.1
20	Co^0	778.3	10	2.19	15.0	–
	Co^{2+}	781.9	90	3.32	15.7	4.6
30	Co^0	778.4	15	2.29	15.0	–
	Co^{2+}	781.6	85	3.13	15.8	4.7

Table 6. Binding energies, relative intensities and FWHMs of different Co species as observed from Co2p of as-deposited and sputtered 1:4 PC Co–W coating prepared at pH5

Duration of sputtering (min)	Co species	E_B of $Co2p_{3/2}$ (eV)	Relative intensity (%)	FWHM of $Co2p_{3/2}$ (eV)	ΔE_B ($2p_{3/2}$–$2p_{1/2}$) (eV)	ΔE_B ($2p_{3/2}$–S) (eV)
As-deposited	Co^0	778.1	9	2.13	15.1	–
	Co^{2+}	781.5	91	2.74	15.5	4.0
10	Co^0	778.3	25	2.02	15.0	–
	Co^{2+}	781.6	75	3.04	15.7	4.4
20	Co^0	778.2	31	2.11	14.9	–
	Co^{2+}	781.7	69	3.35	15.6	4.6
30	Co^0	778.2	37	2.11	15.0	–
	Co^{2+}	781.5	63	2.99	15.8	4.0

Table 7. Binding energies, relative intensities and FWHMs of different W species as observed from W4f of as-deposited and sputtered 1:4 PC Co–W coating prepared at pH8

Duration of sputtering (min)	W species	E_B of $W4f_{7/2}$ (eV)	Relative intensity (%)	FWHM of $W4f_{7/2}$ (eV)
As-deposited	W^0	31.1	8	1.35
	W^{6+}	36.1	92	1.62
10	W^0	31.0	6	1.38
	W^{6+}	36.2	94	1.60
20	W^0	31.0	4	1.32
	W^{6+}	36.3	96	1.55
30	W^0	31.1	2	1.35
	W^{6+}	36.4	98	1.65

Table 8. Binding energies, relative intensities and FWHMs of different W species as observed from W4f of as-deposited and sputtered 1:4 PC Co–W coating prepared at pH5

Duration of sputtering (min)	W species	E_B of $W4f_{7/2}$ (eV)	Relative intensity (%)	FWHM of $W4f_{7/2}$ (eV)
As-deposited	W^{6+}	36.1	100	1.49
10	W^{6+}	36.0	100	1.42
20	W^{6+}	36.0	100	1.52
30	W^{6+}	36.0	100	1.59

Table 9. Relative surface concentrations (at.%) of Co and W evaluated from XPS of various Co–W coatings prepared at pH8 and pH5 with different sputtering conditions

Duration of sputtering (min)	Coatings															
	DC				1:1				1:2				1:4			
	pH8		pH5		pH8		pH5		pH8		pH5		pH8		pH5	
	Co	W	Co	W	Co	W	Co	W	Co	W	Co	W	Co	W	Co	W
As-deposited	94	6	87	13	91	9	91	9	95	5	94	6	92	8	90	10
10	95	5	89	11	91	9	93	7	95	5	95	5	93	7	94	6
20	95	5	89	11	91	9	95	5	96	4	95	5	93	7	94	6
30	95	5	90	10	90	10	92	8	95	5	96	4	94	6	94	6

Table 10. Microhardness of Co−W coatings electrodeposited at pH8 and pH5 with various plating modes

Coatings	Microhardness (HK)	
	pH8	pH5
DC Co−W	369 ± 20	486 ± 20
1:1 PC Co−W	352 ± 20	522 ± 20
1:2 PC Co−W	383 ± 20	503 ± 20
1:4 PC Co−W	367 ± 20	526 ± 20

Figure captions

Figure 1. Pulse electrodeposition profiles of Co–W coatings showing the on-time and off-time in milliseconds (ms).

Figure 2. XRD of as-deposited DC and PC Co–W coatings prepared at pH8 and pH5.

Figure 3. FESEM images of as-deposited Co–W coatings: (a) DC, pH8, (b) 1:2 PC, pH8, (c) DC, pH5 and (d) 1:1 PC, pH5.

Figure 4. DSC profiles of as-deposited DC and PC Co–W coatings prepared at pH8 and pH5.

Figure 5. XPS of core level Co2p of DC Co–W coatings at different stages of sputtering: (a) as-deposited, pH8, (b) after 10 min sputtering, pH8, (c) after 20 min sputtering, pH8, (d) after 30 min sputtering, pH8 and (e) as-deposited, pH5.

Figure 6. Deconvoluted XPS of Co2p of DC Co–W coating prepared at pH8 after 30 min sputtering.

Figure 7. XAES of CoL_3VV of DC Co–W coating prepared at pH8 at different stages of sputtering.

Figure 8. XPS of core level W4f of DC Co–W coatings at different stages of sputtering: (a) as-deposited, pH8, (b) after 10 min sputtering, pH8, (c) after 20 min sputtering, pH8, (d) after 30 min sputtering, pH8 and (e) as-deposited, pH5.

Figure 9. Deconvoluted XPS of W4f of as-deposited DC Co–W coating prepared at pH8.

Figure 10. XPS of core level Co2p of 1:4 PC Co–W coatings at different stages of sputtering: (a) as-deposited, pH8, (b) after 10 min sputtering, pH8, (c) after 20 min sputtering, pH8, (d) after 30 min sputtering, pH8 and (e) as-deposited, pH5.

Figure 11. XPS of O1s of as-deposited DC Co–W coatings obtained from pH8.

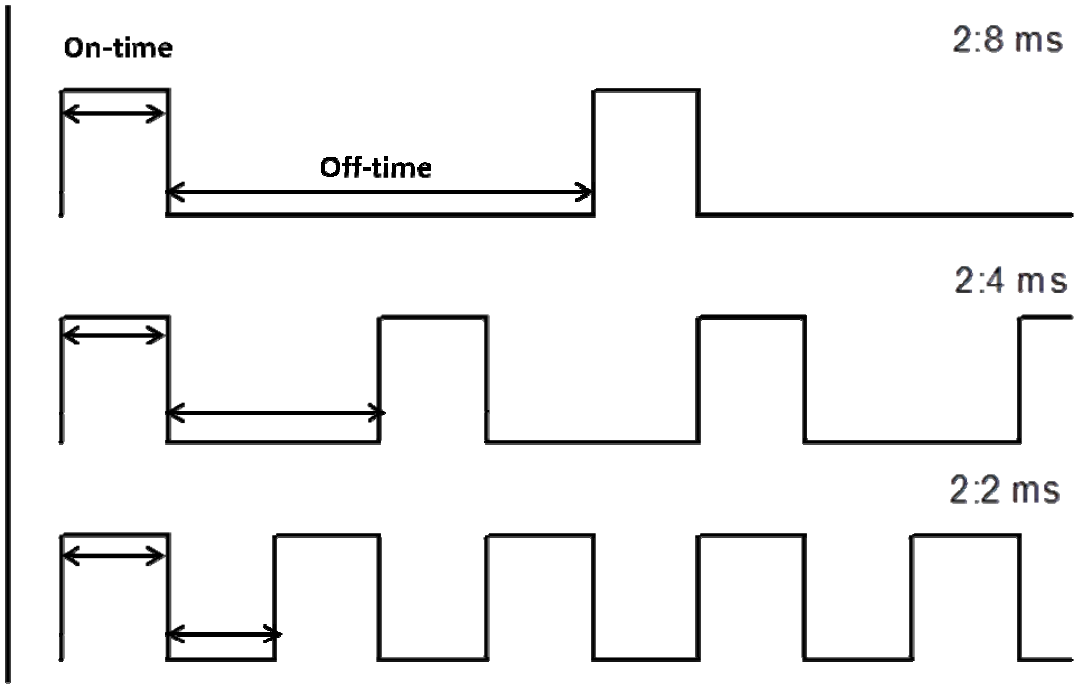

Figure 1. Pulse electrodeposition profiles of Co–W coatings showing the on-time and off-time in milliseconds (ms).

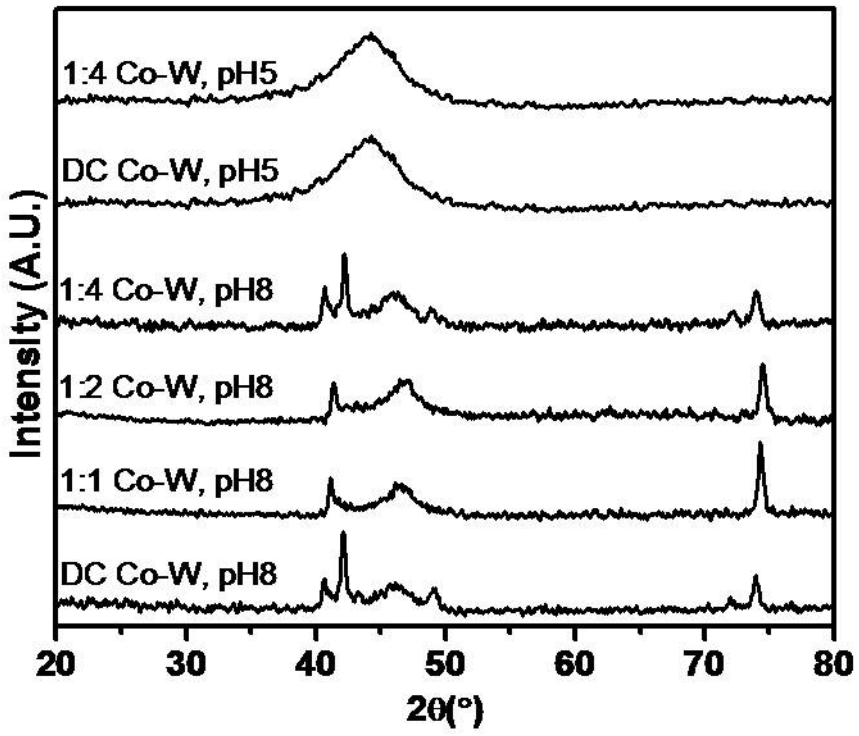

Figure 2. XRD of as-deposited DC and PC Co–W coatings prepared at pH8 and pH5.

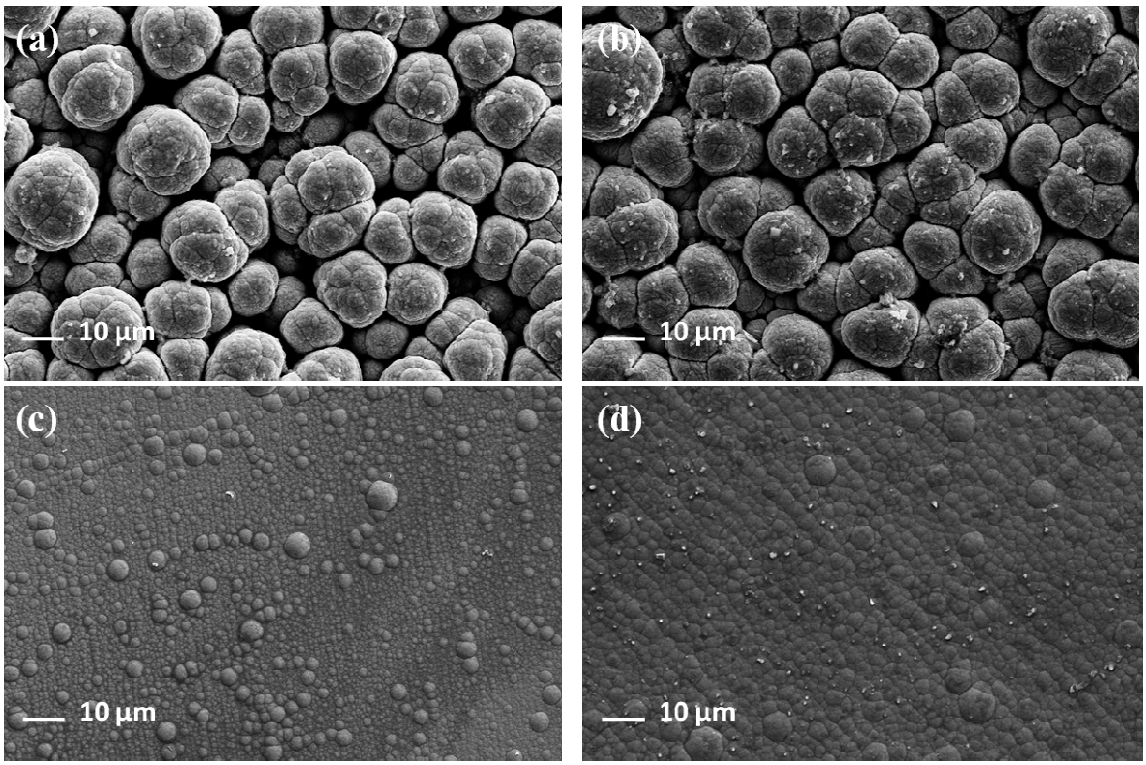

Figure 3. FESEM images of as-deposited Co–W coatings: (a) DC, pH8, (b) 1:2 PC, pH8, (c) DC, pH5 and (d) 1:1 PC, pH5.

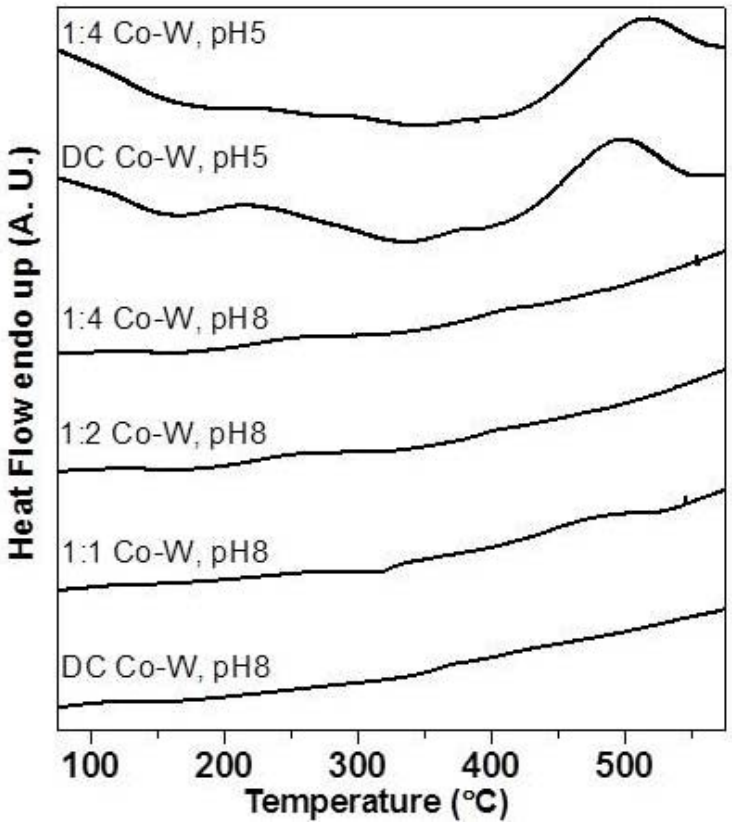

Figure 4. DSC profiles of as-deposited DC and PC Co–W coatings prepared at pH8 and pH5.

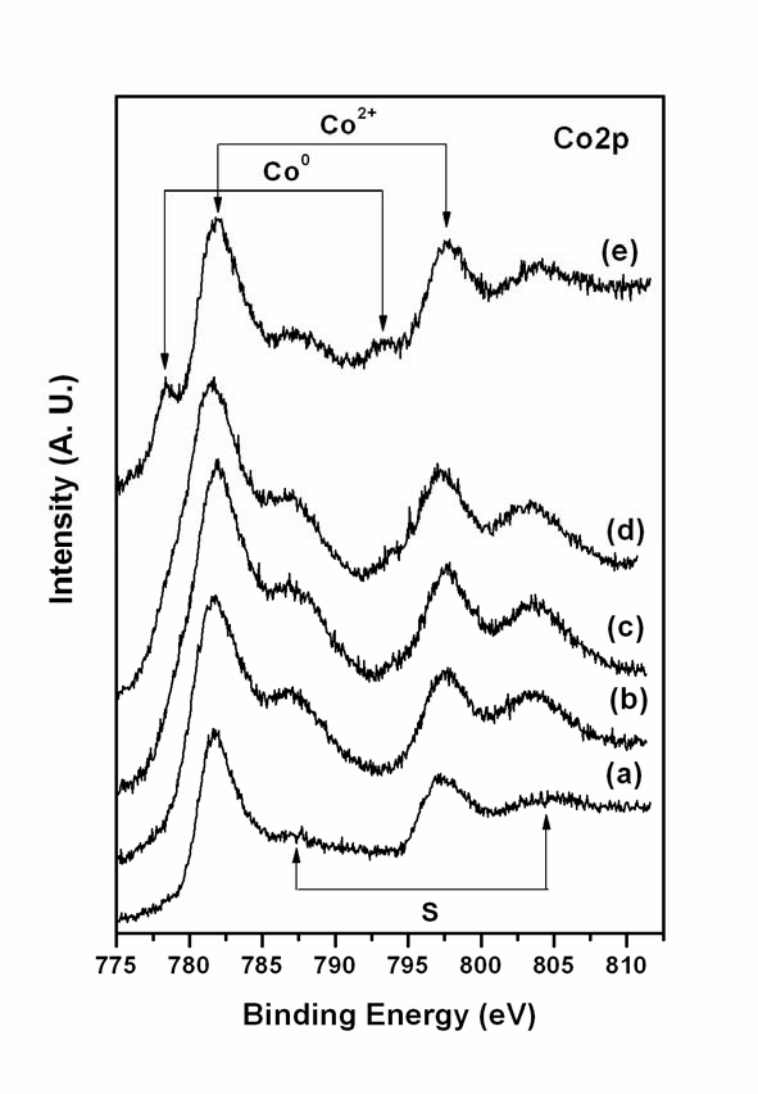

Figure 5. XPS of core level Co2p of DC Co–W coatings at different stages of sputtering: (a) as-deposited, pH8, (b) after 10 min sputtering, pH8, (c) after 20 min sputtering, pH8, (d) after 30 min sputtering, pH8 and (e) as-deposited, pH5.

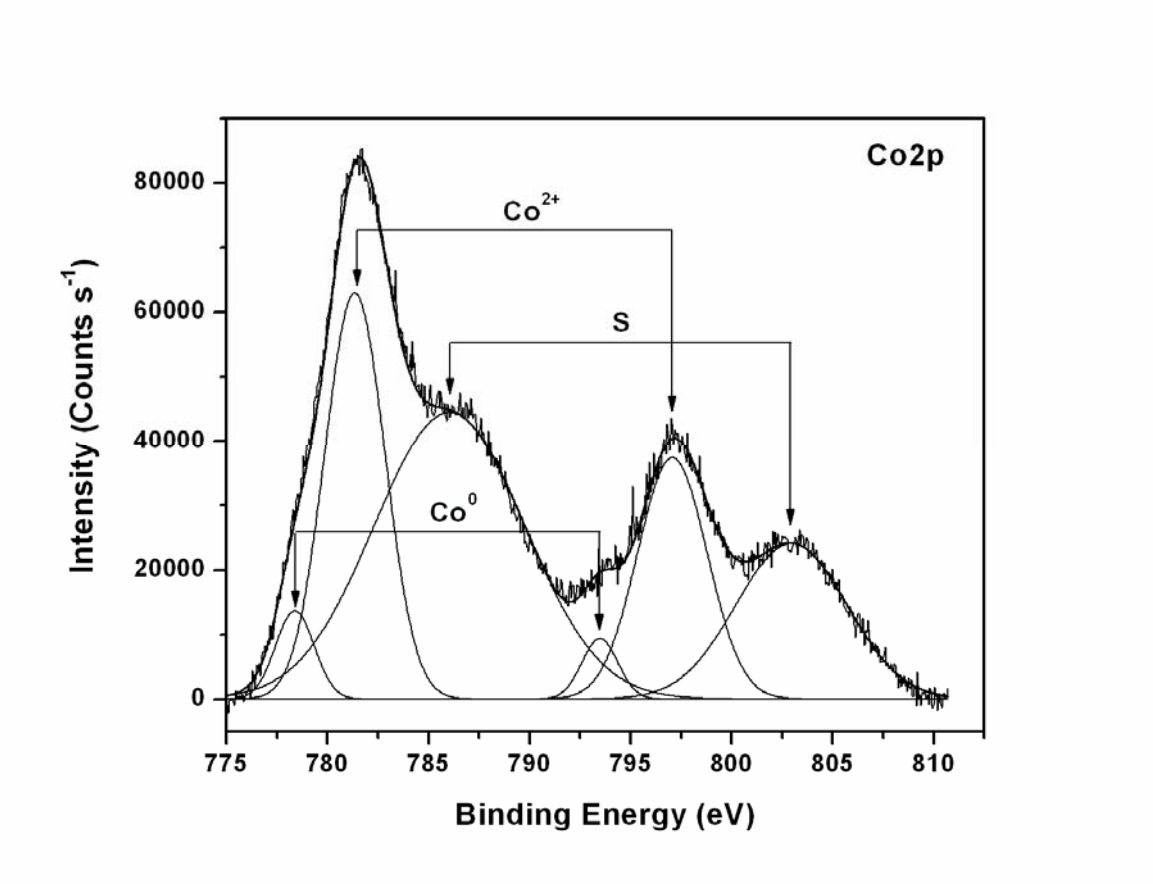

Figure 6. Deconvoluted XPS of Co2p of DC Co–W coating prepared at pH8 after 30 min sputtering.

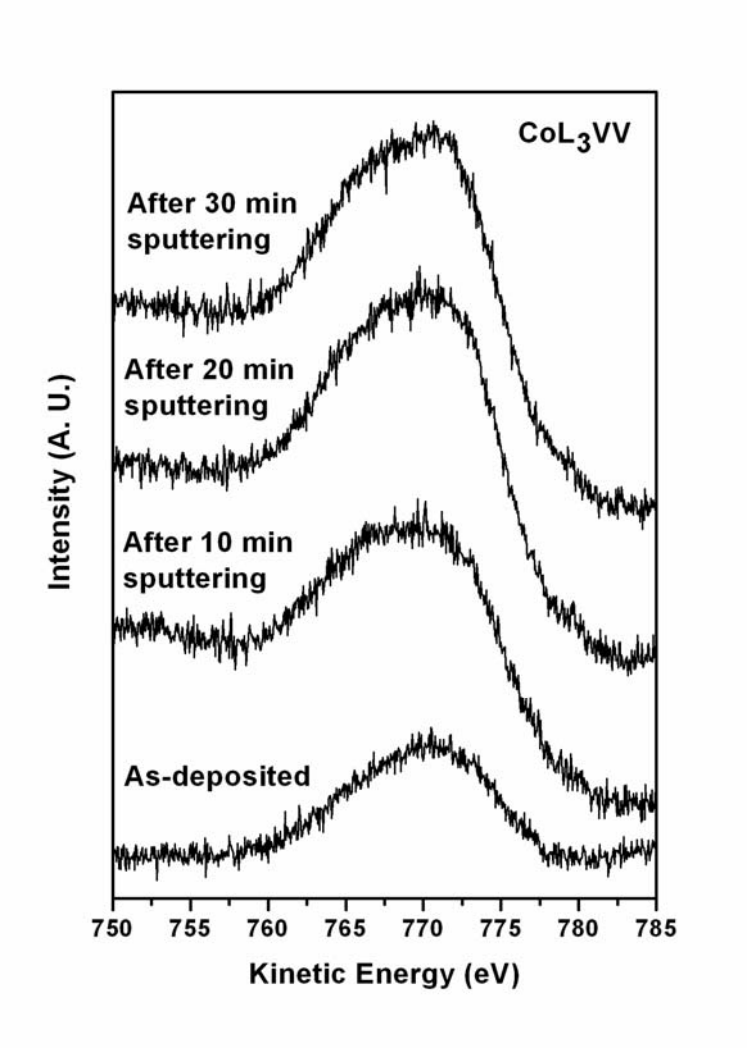

Figure 7. XAES of CoL_3VV of DC Co–W coating prepared at pH8 at different stages of sputtering.

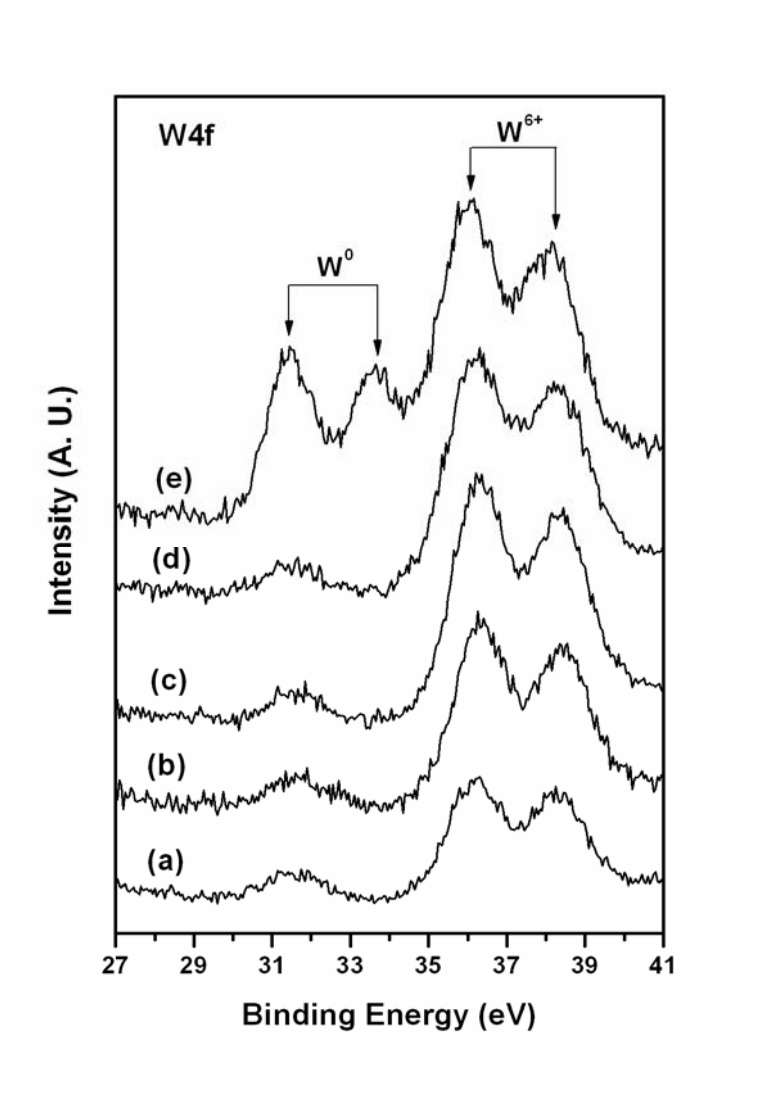

Figure 8. XPS of core level W4f of DC Co–W coatings at different stages of sputtering: (a) as-deposited, pH8, (b) after 10 min sputtering, pH8, (c) after 20 min sputtering, pH8, (d) after 30 min sputtering, pH8 and (e) as-deposited, pH5.

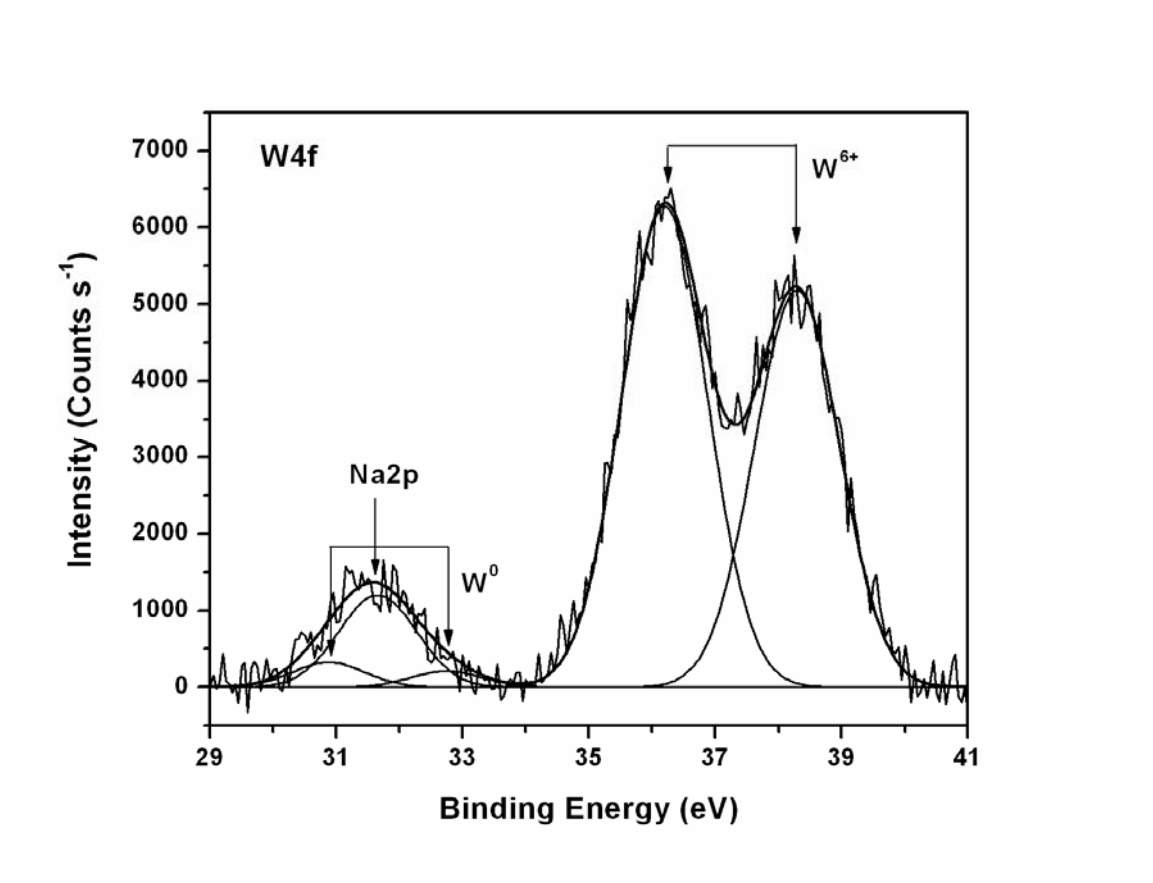

Figure 9. Deconvoluted XPS of W4f of as-deposited DC Co–W coating prepared at pH8.

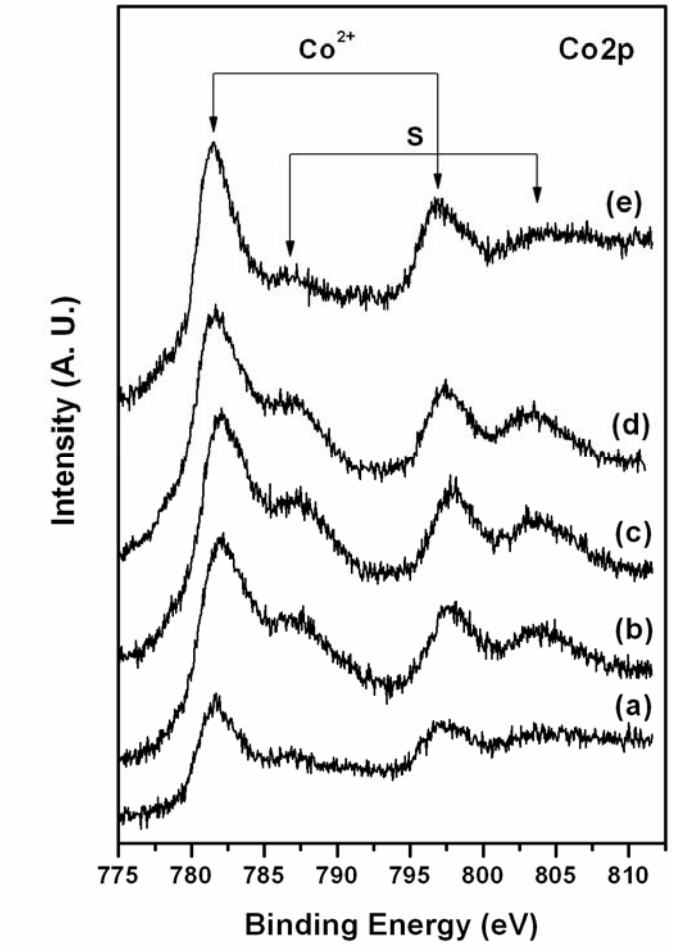

Figure 10. XPS of core level Co2p of 1:4 PC Co–W coatings at different stages of sputtering: (a) as-deposited, pH8, (b) after 10 min sputtering, pH8, (c) after 20 min sputtering, pH8, (d) after 30 min sputtering, pH8 and (e) as-deposited, pH5.

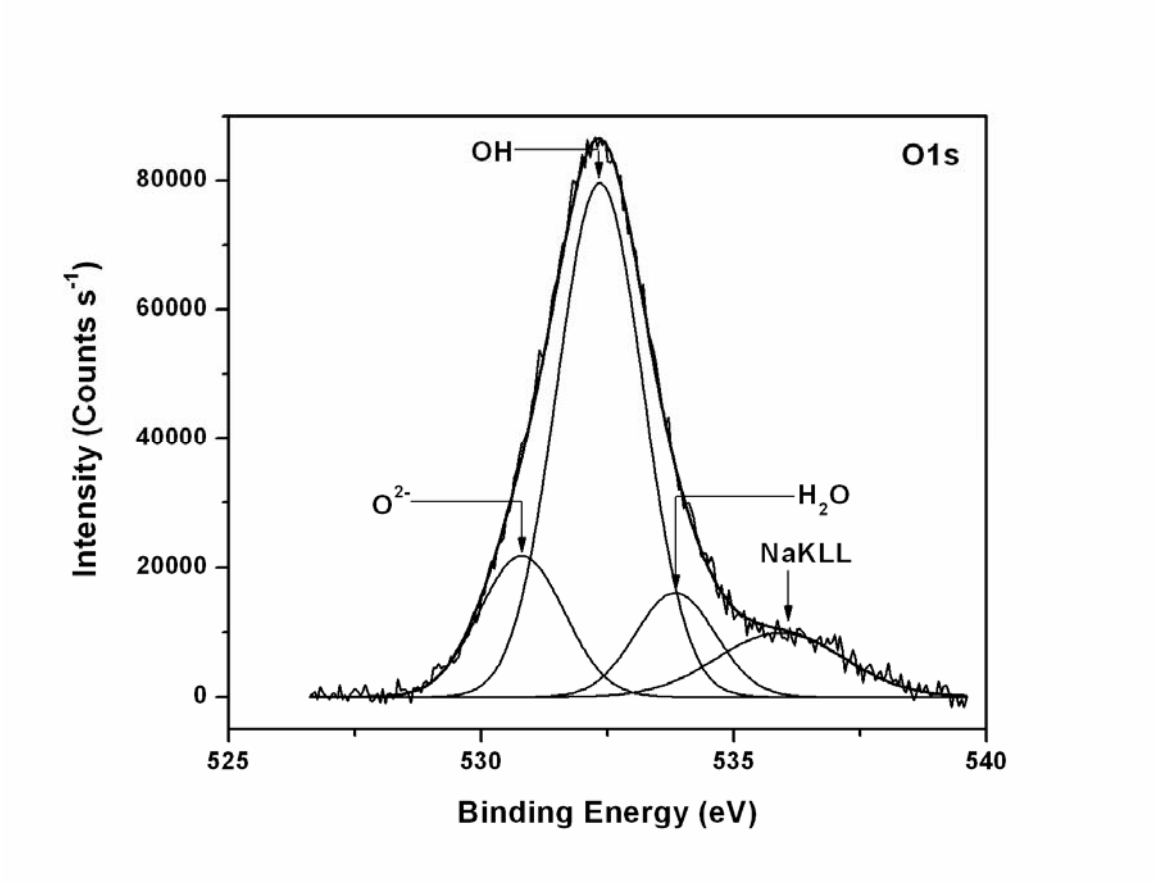

Figure 11. XPS of core level O1s of as-deposited DC Co–W coatings obtained from pH8.